Heliyon 8 (2023) e12512

Contents lists available at ScienceDirect

Heliyon

journal homepage: www.cell.com/heliyon

Research article

Gefitinib conjugated PEG passivated graphene quantum dots incorporated PLA microspheres for targeted anticancer drug delivery

Abhishek Gautam [a], Kaushik Pal [a,b,*]

[a] Centre for Nanotechnology, Indian Institute of Technology Roorkee, Roorkee, 247667, India
[b] Department of Mechanical and Industrial Engineering, Indian Institute of Technology Roorkee, Roorkee, 247667, India

GRAPHICAL ABSTRACT

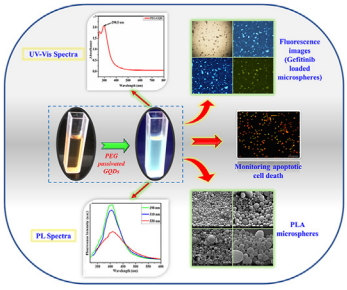

ARTICLE INFO

Keywords:
Graphene quantum dots (GQDs)
PLA
Gefitinib
Targeted drug delivery
Lung cancer

ABSTRACT

In the present study, polyethylene Glycol passivated Graphene Quantum Dots (PEG-GQDs) were successfully synthesized via the hydrothermal method. Furthermore, for the synthesis of anticancer drug loaded GQD embedded microspheres, the anticancer drug was mixed with synthesized PEG-GQD. As prepared, Gefitinib-PEG-GQDs were incorporated into poly-lactic acid (PLA) microspheres using poly-vinyl-acetate (PVA) as surfactant via solvent evaporation technique and single emulsification method. The successful synthesis of anticancer drug loaded microspheres was confirmed by several characterization techniques, including Field-Emission Scanning Electron Microscopy (FE-SEM), which shows the morphology of microspheres, Fourier Transform Infrared Spectroscopy (FTIR) analysis gives an idea about functional group present in the microspheres. X-ray diffraction (XRD) provides information about the crystallinity of the samples respectively. The drug release characteristics were determined by UV-Vis spectrophotometric analysis. Moreover, the *in-vitro* cell-based cytotoxicity assay indicated almost insignificant cytotoxicity of the NCI–H522 cell line (Human, Lung, Non-small cell lung cancer).

1. Introduction

Lung cancer is the leading cause of cancer-related death globally [1]. Chemotherapy is currently the most widely used cancer treatment, and it is based on the systematic giving of bolus medicines to cancer patients [2]. In any case, the major complication that decelerates effective drug accumulation is the multidrug resistance of cancer cells. Combinatorial treatment, including different drugs or potential drug applicants having unique signaling pathways, enhanced remedial impacts against particular targets, and intends to defeat components of protection, is a promising alternative

* Corresponding author.
E-mail address: pl_kshk@yahoo.co.in (K. Pal).

https://doi.org/10.1016/j.heliyon.2022.e12512
Received 26 April 2022; Received in revised form 20 July 2022; Accepted 14 December 2022

to chemotherapy administered by a single specialist [3]. This way, nanotechnology-mediated delivery of anticancer drugs inside a single treatment platform can be a successful technique and it can be validated by using computed tomography (CT) images [3, 4].

Nanotechnology holds significant assurance for solving these difficulties by empowering a lot of therapeutic drugs to be encapsulated into nanoparticles. Moreover, it expands the half-life of the drug, diminishes lethal unfavorable effects related to the drug, and enhances its pharmacokinetic profile and therapeutic efficiency [5, 6].

Drug delivery system which is inexplicable in delivering the particular drug to a patient. In drug delivery the drug is absorbed across a biological membrane, whereas the drug is released in a dosage form in this system. This system is based on a process that delivers a certain quantity of a therapeutic agent for an extended period to a targeted diseased area within the body. It's also a feasible way to increase the effective use of a drug and minimalize adverse side effects and toxicity [7, 8]. Polymer-based nanoscale drug delivery systems (DDSs) as 'nanomedicines' have received a lot of attention in recent decades for chemotherapeutic drug delivery in cancer treatment. They provide biocompatibility, controlled drug release profiles, increased circulation times, and accumulation at the cancer site due to enhanced permeability and retention (EPR) effects with an appropriate outline and basic adaptability [9, 10, 11].

Transporting therapeutic agents to the desired site at the appropriate moment is the fundamental difficulty in drug delivery. In addition to symptoms and lethality, oral-regulated anticancer medications or infusions suffer from the adverse effects of constrained control on drug release rate. For a more extended period, the preferred regimen is a robust initial medication release followed by a progressive decrease over time [12]. The regulated distribution of medicine is a viable option for overcoming the limitations mentioned earlier and allowing the drug to be released continuously. In controlled drug delivery, first-order kinetics may be used to achieve an optimal and effective drug concentration at the target region, followed by zero-order kinetic. This type of release mechanism is made possible by conjugating the drug to a polymer that allows for controlled release. In any event, the polymer should be biodegradable and wiped out by the physiological system without leaving residues that could collect in cell compartments, such as liposomes or tissues from the phagocytosis system [13].

Because of their ability to encapsulate a variety of medications, biocompatibility, high bioavailability, and prolonged drug release characteristics, polymeric microspheres are attractive carriers for a variety of controlled delivery applications. It's likewise a practical method to expand the successful utilization of a drug and minimalize undesirable symptoms and toxicity [14, 15, 16]. Designing methods for combining imaging tools with anticancer drugs-carrying microspheres for concurrent intracellular tracking and therapy opens up a new and more significant avenue for cancer treatment. The most recent members of the family of luminous carbon nanomaterials are Graphene quantum dots (GQDs) with zero dimension [17]. In comparison to traditional dyes and poisonous semiconductors, quantum dots are well known for their strong fluorescence, surface modification flexibility, high solubility, chemical inertness, ease of production, excellent biocompatibility, high photostability, and low toxicity [18, 19]. Graphene quantum dots' remarkable properties make them ideal for bioimaging applications. We recently used the hydrothermal approach to make luminous GQDs and used them for bioimaging in cancer cells [16]. For this, we have used poly (ethylene glycol) (PEG) as a carbon source and ethanol as a solvent because of its good solubility for anticancer drugs. Here, PEG is utilized to enhance the fluorescence properties of graphene quantum dots by passivating their surfaces. These biocompatible PEG-GQDs can be used to label cancer cells with green fluorescence in conjunction with drugs because of their high fluorescence and excellent photostability [20].

PEG-GQDs act as a promising tool in cancer therapy. It has been found that PEG modifications facilitated NPs internalization into the cells [21]. Because of their Nano size, they increase the surface area for drug dissolution in the microsphere and also increase the drug loading efficiency [22, 23, 24].

Here, we are using PLA as a polymer matrix to encapsulate drugs because of its good biodegradability and biocompatibility. Additionally, the release profile of the drug can be controlled after being encapsulated into PLA [25]. Nowadays, the Gefitinib drug is widely used to treat lung

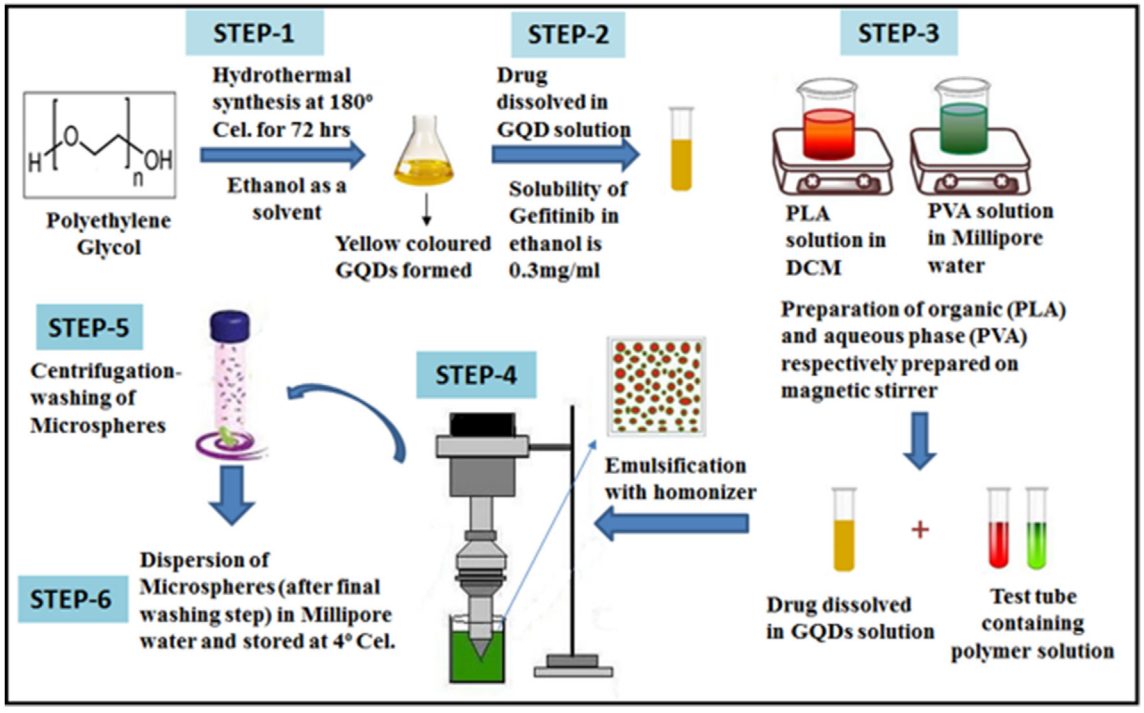

Figure 1. Schematic view of preparation of anticancer drug loaded microsphere.

cancer. It is extensively metabolized in the liver, predominantly by cytochrome P450 (CYP) 3A4 [26, 27].

Gefitinib is a low atomic weight inhibitor of the intracellular tyrosine kinase space of the epidermal development factor receptor. It has been noteworthy in the treatment of Non-small cell lung cancer and has been affirmed by the Food and Drug Administration (FDA) in 2015 as the mainline treatment for patients with an epidermal development factor receptor change and Non-small cell lung cancer [28]. Notwithstanding, as an oral medication, the remedial window of Gefitinib is minimal because of its poor solubility in aqueous solvents with pH $>$ 7, which brings about poor bioavailability. A high dose is then required amid clinical use of Gefitinib in view of its poor aqueous solubility, which may prompt extra dangerous responses and adverse impacts [29, 30].

As high drug concentration causes cancer cells to develop resistance property against the drug, resulting in the failure of chemotherapy. Thus, to increase the efficacy of drug, and to maintain the sustained and controlled release behaviour of the chemotherapeutic agent towards lung cancer, we conjugated gefitinib to the graphene quantum dots and encapsulated in the PLA microspheres for simultaneous imaging and drug delivery for the ablation of lung cancer cells. The main aim of our study was to prepare a microsphere/quantum dots arrangement that will be used for controlled delivery of an anticancer drug, i.e., Gefitinib, which eliminates the initial burst and can track the accumulation of the drug in lungs by using a mixture of PLA microspheres and self-passivated PEG-GQDs to provide controlled release of Gefitinib for over a prolonged period of time. Earlier no reports on the functionalization of graphene quantum dots with anticancer drug, gefitinib is reported. Therefore, gefitinib conjugated graphene quantum dots encapsulated in PLA microspheres prepared in this work can be good candidates for cell imaging and drug delivery. Overall, it is anticipated that the innovative DDS will be a great alternative for cancer therapy.

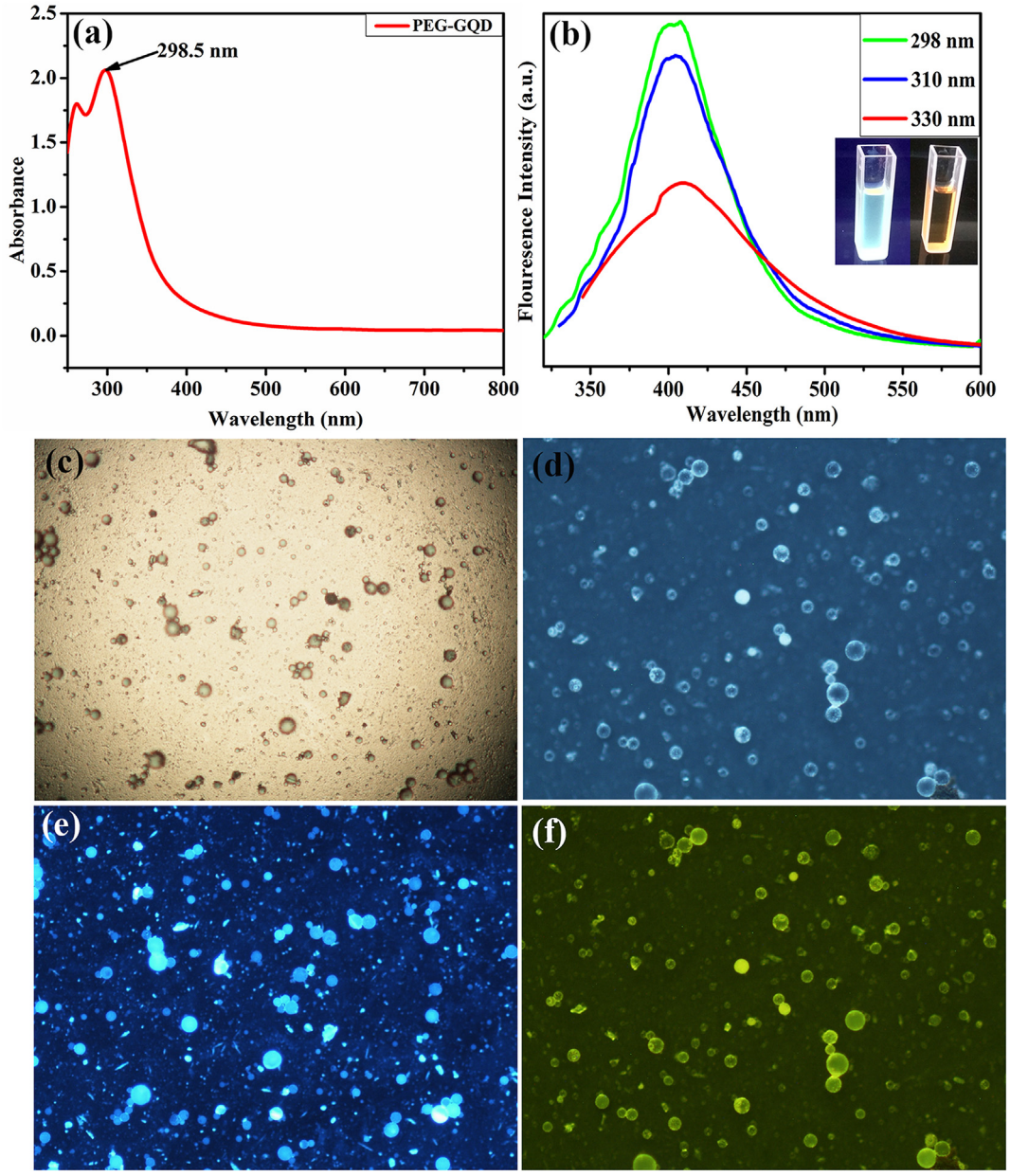

Figure 2. (a) UV-Visible spectra of PEG-GQDs, (b) PL spectra of PEG-GQDs at the different excitation wavelengths (inset: GQD solution under UV light and Visible light, next are Fluorescence microscopy images of Gefitinib loaded microspheres (c) Without filter under bright field, (d) dark filter, (e) Microspheres showing blue fluorescence under the green filter, (f) Microspheres showing green fluorescence under the blue filter.

2. Experimental section

2.1. Materials

Poly (lactic acid) (PLA) (MW 2 * 104 g/mol) was purchased from Sigma Aldrich, Poly (vinyl alcohol) (PVA) (MW86.09 g/mol), Dichloromethane (DCM) (MW 84.93) and Poly (ethylene glycol) (PEG) (MW 62.068 g/mol) were taken from Himedia Laboratories, India. Ethanol (absolute) (MW 46.07) was imported from Changshu Hongsheng Fine Chemical Co., Ltd. Gefitinib Tablets IP 250 mg was purchased from SAMARTH Life Sciences Pvt. Ltd. National Centre for Cell Science (NCCS), Pune, provided the NCI–H522 cell line (Human, Lung, Non-small cell lung cancer) for this study. Penicillin/Streptomycin antibiotic, 3-(4,5- dimethyl-2-thiazolyl)-2,5-diphenyl-2H-tetrazolium bromide (MTT), Ethanol (EtOH), Phosphate-buffered saline (PBS), dimethyl sulfoxide (DMSO) cell culture grade (≥99.8%), Dulbecco's modified Eagle's medium (DMEM), Fetal bovine serum (FBS), 98% sodium hydroxide pellets (NaOH), and the trypsin-EDTA solution was brought from HiMedia Laboratories Pvt. Ltd., India. All of the tissue culture flasks and tissue culture plates were supplied by HiMedia Laboratories Pvt. Ltd., Mumbai (India).

2.2. Characterization techniques and instruments used

Samples morphology of Gefitinib loaded GQD embedded microspheres was observed by Field Emission Scanning Electron Microscopy (FESEM), using a Zeiss-Ultra Plus field emission microscope, and for PEG-GQDs, the sample morphology and size were analyzed by using the HRTEM instrument at operating voltage of 200kV. For detection of functional groups present in PEG-GQDs, Fourier Transform Infrared spectroscopy (FT-IR) was executed using a Thermo Scientific Nicolet 6700 FT-IR spectrometer. Zeta potential was measured to check the colloidal stability using a Malvern Zeta Potential Sizer Nano ZS 90. The absorption property of Gefitinib-loaded microspheres was analyzed by using Lasany LI-2800, a UV−vis spectrophotometer. To measure the fluorescence property of Gefitinib-loaded microspheres, fluorescence spectrophotometry was done with F-4600 FL Spectrophotometer, and fluorescence microscopy was done by using a Nikon Eclipse LV100 fluorescence microscope. To determine the crystallinity of the sample, the XRD pattern was captured using a Bruker AXS D8 Advance powder X-ray diffractometer with a Cu tube (= 1.5409 A°) in the angle range of 5°–80° with a 0.1°/min increment.

2.3. Synthesis of graphene quantum dots

15 gm PEG was dissolved in 50 ml of ethanol (absolute) and stirred for 1 h. The resulting solution was transferred to Teflon-lined autoclaved for 72 h at 180 °C. Finally, a yellow-colored solution of PEG-passivated graphene quantum dots (PEG-GQDs) was collected. A prepared sample has been used for various characterization and further synthesis protocols.

2.4. Gefitinib loading in graphene quantum dots

The solubility of Gefitinib in Ethanol is 0.3 mg/ml. So, we have prepared GQDs in ethanol itself to achieve good adhesion of medicine with the GQDs by directly dissolving Gefitinib into PEG-GQDs solution in ethanol. Primarily Gefitinib was mixed with PEG-GQDs solution in ethanol and stirred for 2 h to dissolve the drug into PEG-GQDs incorporated ethanol solution. Furthermore, this solution was kept at room temperature (28 °C) for 24 h to remove ethanol for further processing. After 24 h, the drug molecule conjugated PEG-GQD was synthesized successfully.

The (% LC) drug loading capacity and (% EE) encapsulation efficiency of Gefitinib in the PEG-GQDs incorporated microsphere was calculated by UV–vis spectrophotometer.

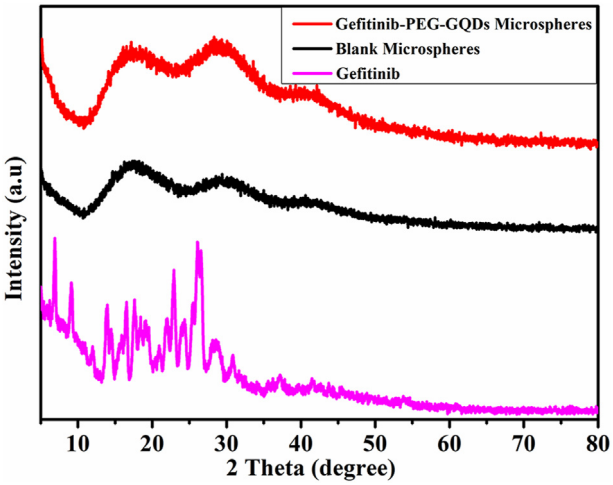

Figure 3. X-ray diffraction patterns of Gefitinib, Blank PLA/PVA microspheres, and Gefitinib-loaded GQD embedded microspheres.

The following equations were used to measure the loading capacity and encapsulation efficiency of the drug:

$$LC = \frac{Total\ \ amount\ \ of\ \ drug - Free\ \ amount\ \ of\ \ drug}{Weight\ \ of\ \ dried\ \ nanocarrier} \times 100 \quad (1)$$

$$EE = \frac{Total\ \ amount\ \ of\ \ drug - Free\ \ amount\ \ of\ \ drug}{Total\ \ amount\ \ of\ \ drug} \times 100 \quad (2)$$

2.5. Synthesis of gefitinib conjugated PEG-GQD incorporated microsphere

We have synthesized Gefitinib-PEG-GQD incorporated microsphere via the technique reported by Barkha. et al. [31] with minor modification as shown in Figure 1. In the typical synthesis method, 5 ml of 2.5% w/v PLA solution in DCM and 10 ml of 2.5% w/v of PVA in DI water were prepared by stirring the solutions for several hours. Furthermore, the PLA solution was mixed with 1.5 mg of Gefitinib- PEG-GQD. The solution was stirred for 1 h for complete dispersion of Gefitinib-PEG-GQD into PLA solution as the prepared solution was further used for emulsification and preparation of the microsphere. Typically, this solution was kept on sonication, and during the sonication process, PVA solution was added slowly to form the emulsion until the whole PVA solution was consumed. Furthermore, 10 ml DI water was added, and sonication was continued for the next ten more minutes. After that, as prepared emulsion was

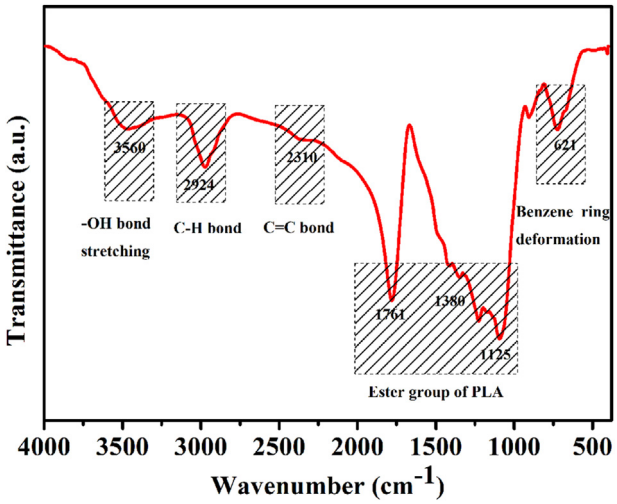

Figure 4. FT-IR spectra of drug-loaded microsphere.

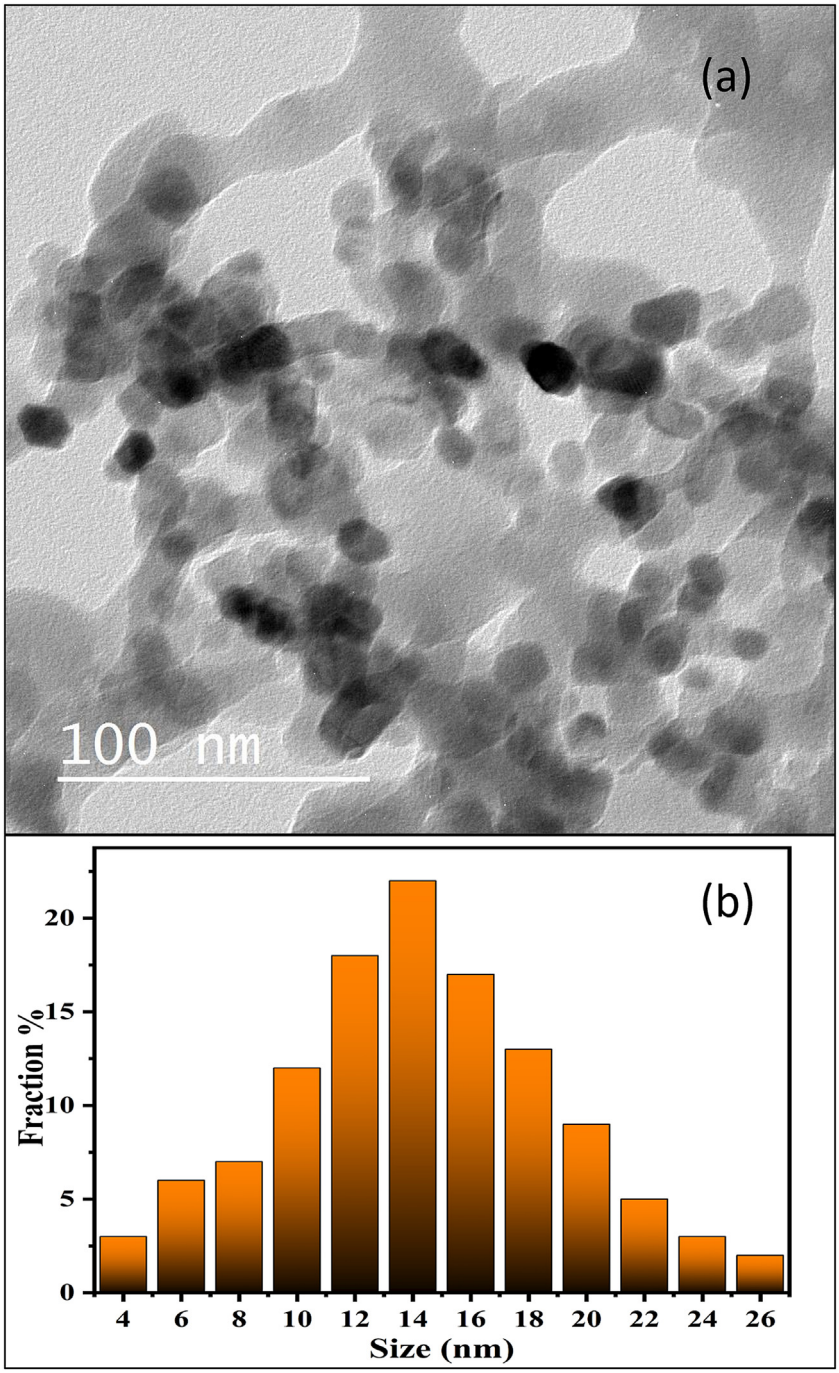

Figure 5. HRTEM images of graphene quantum dots.

transferred to the stirrer and left for stirring overnight for the excess solvent evaporation. As prepared microsphere was washed using a centrifuge for the removal of surfactant. Specifically, washing was done three times at 6000 rpm at a temperature of 4 °C for 15 min. After washing, microspheres were dispersed into the distilled water and stored at 4 °C till further characterization.

2.6. Cytotoxicity assay to check the biocompatibility of anticancer drug loaded microspheres

Cytotoxicity assay, also called MTT assay, is based on the action of the enzyme, i.e., cellular mitochondrial oxido-reductase. For estimation of cell viability, the sample obtained at different stages of preparation of microspheres and the final sample of anticancer drug loaded microsphere sample were firstly sterilized by UV light exposure, and then these cells were seeded over them in 96 well plate, and for next 48 h, they are allowed to grow on it. As the desirable time period was completed, the culture medium was discarded from every single well, and cells were seeded over all different samples. Then the cells were subjected to incubation with 0.5 mg/mL of MTT reagent for 4 h at 37 °C and put inside the CO_2 incubator under the desirable dark conditions. After the 48 h of incubation is completed, the absorbance of blue color, which is the consequence of solubilization of water insoluble formazan crystal in DMSO, is used to calculate cell viability. When they begin converting MTT salt in the presence of mitochondrial dehydrogenase enzymes present inside the cells, the solubilized salt will turn blue in colour. We may conclude that this cell viability assay focusing on MTT distinguishes between live and dead cells since, in the presence of an enzyme, only

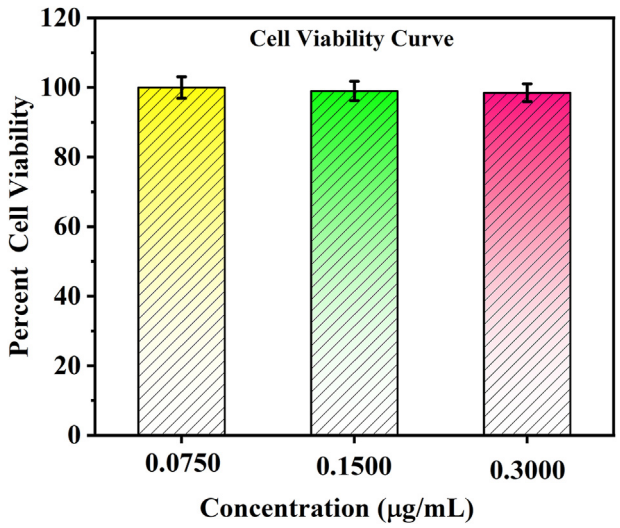

Figure 6. PEG passivated quantum dots in ethanol.

viable cells will convert the salt into formazan crystal. The final absorbance of the solution was determined at 585 nm by using BMG Labtech FLUOstar OPTIMA. All the collected samples were further tested in triplet sets.

2.7. Degradation study of microspheres

The microsphere degradation study was done to determine the pattern for drug release and to examine the changes in the morphology of microspheres. The sample was dissolved in standard 1X PBS solution and then was kept on a stirrer for 20 days. The sample was collected at time intervals and was prepared for the FESEM analysis.

2.8. Drug release study of microspheres

The release of Gefitinib from drug-loaded microspheres was calculated over an unlike pH environment using the dialysis bag method via UV-Vis spectroscopy analysis. In this process, we have used two different buffer solutions, acetate buffer (10 mM, pH 4.5) and PBS (10 mM, pH 7.4), respectively. To calculate the release profile of Gefitinib, 2 mL dispersion of Gefitinib-PEG-GQD microspheres solution was kept in two different dialysis bags, and these bags were suspended into the two separate beakers containing 50 ml of acetate buffer and PBS buffers respectively. Both beakers were kept on stirring at 100 rpm speed, and a small amount of Gefitinib-PEG-GQD microspheres from both the beakers was after 2, 4, 6, 8, 10, 12, 24, 36, 48 h, five days, and ten days, respectively as collected samples were taken to UV-Vis spectrophotometer for absorbance analysis. The absorption of Gefitinib was predicted from the dose-absorption curve of Gefitinib. The Gefitinib released was calculated in percentage form by the following formulae:

$$Gefitinib\ \ release\ (\%) = \frac{Gefitinib\ \ released\ \ in\ \ medium \times 100}{Gefitinib\ \ loaded\ \ in\ \ microspheres} \quad (3)$$

Table 1. IC 50 value of the drug in various composition.

Drug composition	IC50 Value µg/ml
Drug + PEG in EtOH	2.909
Drug in EtOH	2.784
FINAL SAMPLE	1.210

2.9. Statistical analysis

All experimental protocols were repeated thrice. The student's t-test and the Mean ± S.D. were used to determine the significance of the data. GraphPad Prism software 5.0 (GraphPad Inc., CA, USA), and Origin 2019b was used to calculate the statistical treatment of data, with $p < 0.05$ being considered to be statistically significant.

3. Results & discussion

3.1. Optical characterizations

The absorbance of PEG-GQDs in Ethanol is recorded by scanning in the range from 200 to 800 nm. The maximum excitation wavelengths were measured at 298 nm Figure 2(a) shows absorption characteristics peaks of the GQDs. The most prominent peak is located at 298.5 nm, similar to other reported work. In Figure 2(b), The Fluorescence spectroscopy analysis shows that the emission wavelengths were recorded from 315 to 700 nm. The maximum emission was measured at 404 nm, which corresponds to a violet color in the VIBGYOR spectra. Excellent optical properties of graphene quantum dots are suggested due to the presence of carboxyl or hydroxyl groups in PEG-passivized GQDs. Figure 2(b) also demonstrates the fluorescence range of GQDs at various excitation wavelengths at room temperature. Maximum emission was observed at 405 nm under an excitation wavelength of 298.5 nm, which falls into the retention band of PEG-GQDs. Moreover, as the excitation wavelength changed from 298 to 330 nm, the PL peak shifted from 405 to 420 nm. The position of the maximum of the emission is dependent on the excitation wavelength.

Figure 2(c), (d). (e), (f) showing the fluorescence microscopy micrographs of Gefitinib loaded and GQDs embedded microspheres showing fluorescence under different filters proving the GQDs labeling in drug loaded microspheres at 10× magnification.

3.2. X-ray diffraction analysis

The structure of Gefitinib, Gefitinib loaded GQD embedded microspheres, and blank PLA/PVA microspheres were investigated by a pattern produced by X-Ray diffraction (XRD), as shown in Figure 3 Gefitinib shown five diffraction peaks at $2\Theta = 18.6°$, 19.2°,24.2°, 26.2° and 26.4° due to its high crystalline nature.

The blank PLA/PVA microspheres don't show any distinguish peak except one broad, most prominent peak at $2\Theta = 16.5°$; hence it can be concluded that PLA is amorphous in nature. Moreover, Gefitinib-PEG-GQDs microspheres also do not show any detectable peaks regarding Gefitinib loading because the amount of drug is well below the detection limit of XRD.

3.3. Fourier transform infrared spectroscopy analysis

The FT-IR spectroscopy measurement, as shown in Figure 4 of the Gefitinib-PEG-GQDs microsphere sample, has exhibited various absorption bands. The FT-IR spectrum of drug-loaded graphene quantum dots microsphere shows a characteristic peak of benzene ring deformation at 621 cm^{-1}. Three absorption bands at 1125, 1380, and 1761 cm^{-1}, represent the spine ester group of PLA.

The peak at 2310 cm^{-1} shows C=C is due to aromatic ring stretching in the polymer backbone. The peak at 2924 cm^{-1} is related to the symmetric modes of the C–H bond. Peaks at ~ 3500–2500 cm^{-1} are related to the O–H bond stretching of Carboxylic acid. The –OH stretching mode is also visible in spectra at 3560 cm^{-1}. The broad peak is due to moisture content present in the sample [32, 33, 34, 35]. Because the Gefitinib is entrapped into the core of the nanoparticles, due to this reason, the characteristic peak of the secondary amine group (–NH, 3398 cm^{-1}) from standard Gefitinib is not prominent here.

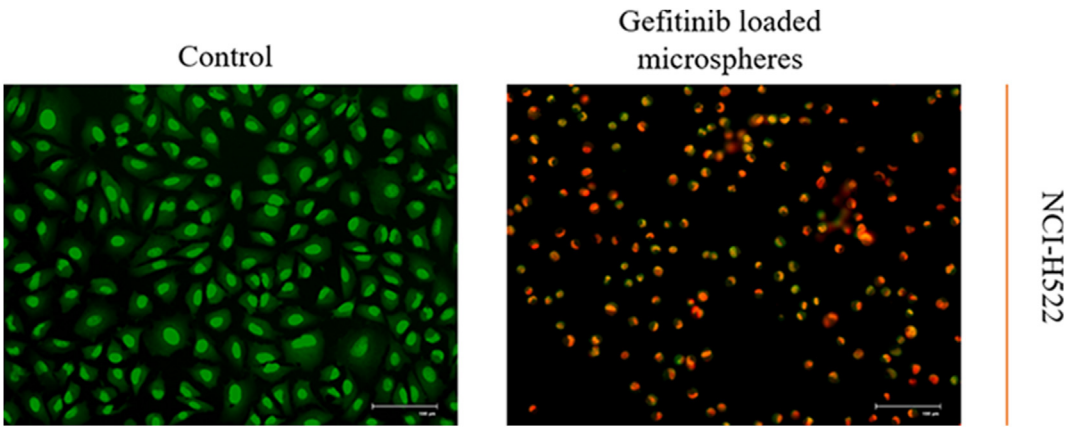

Figure 7. AO/EtBr fluorescent stained NCI–H522 cell images treated with IC_{50} value.

3.4. Transmission electron microscope analysis

In Figure 5 TEM image analysis of the PEG-GQDs prepared via hydrothermal method showed that the graphene quantum dots are almost equally dispersed with a consistent diameter of 4–26 nm, and the average diameter calculated by histogram is nearly 13 nm.

3.5. MTT assay analysis

The cell-viability of PEG-GQDs and Gefitinib showed excellent values. It confirms the low cytotoxicity and biocompatibility of both the materials, and they can be used on the living cell. This has also been proved with the evaluation of cell death.

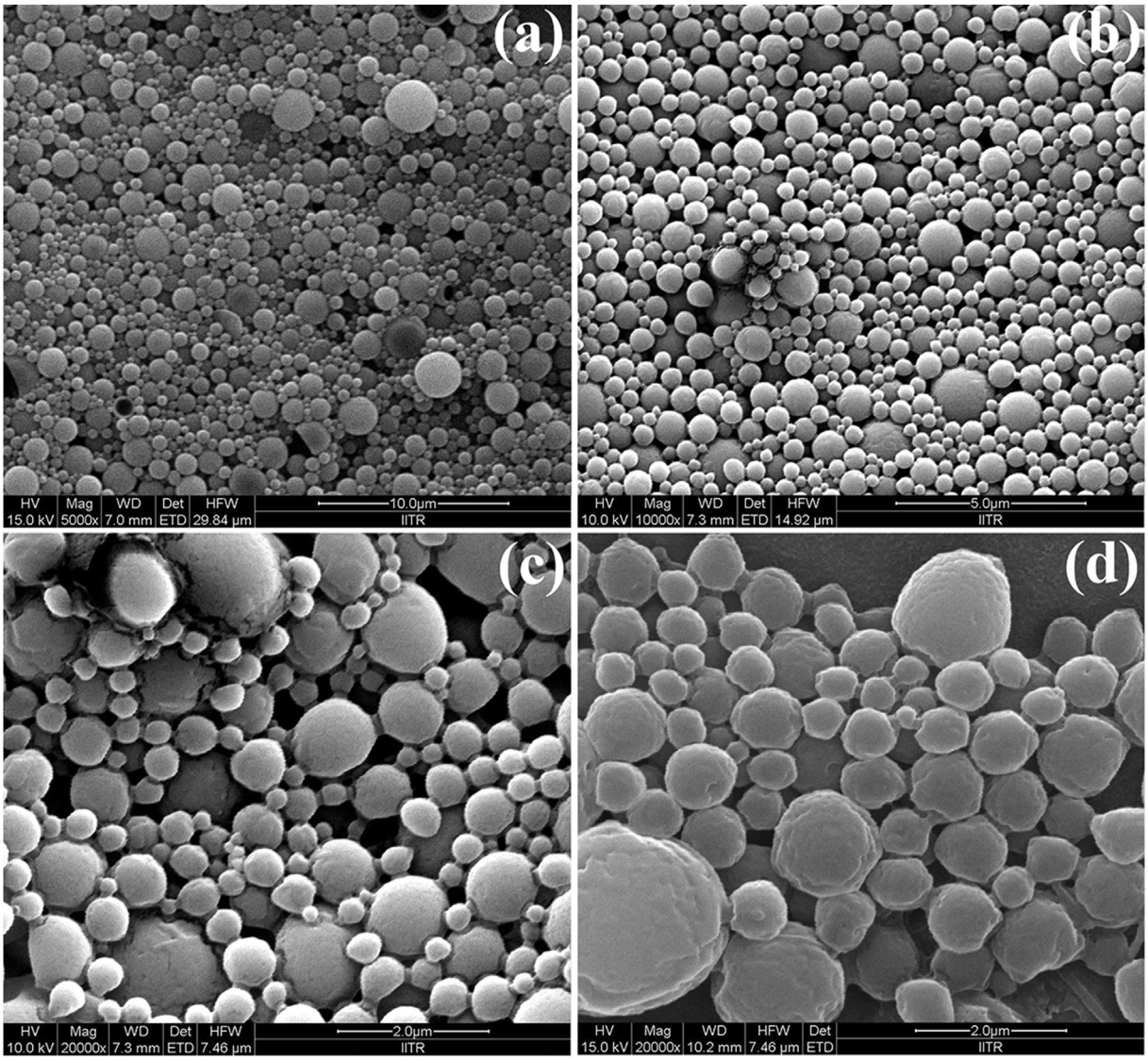

Figure 8. FESEM image of a microspheres.

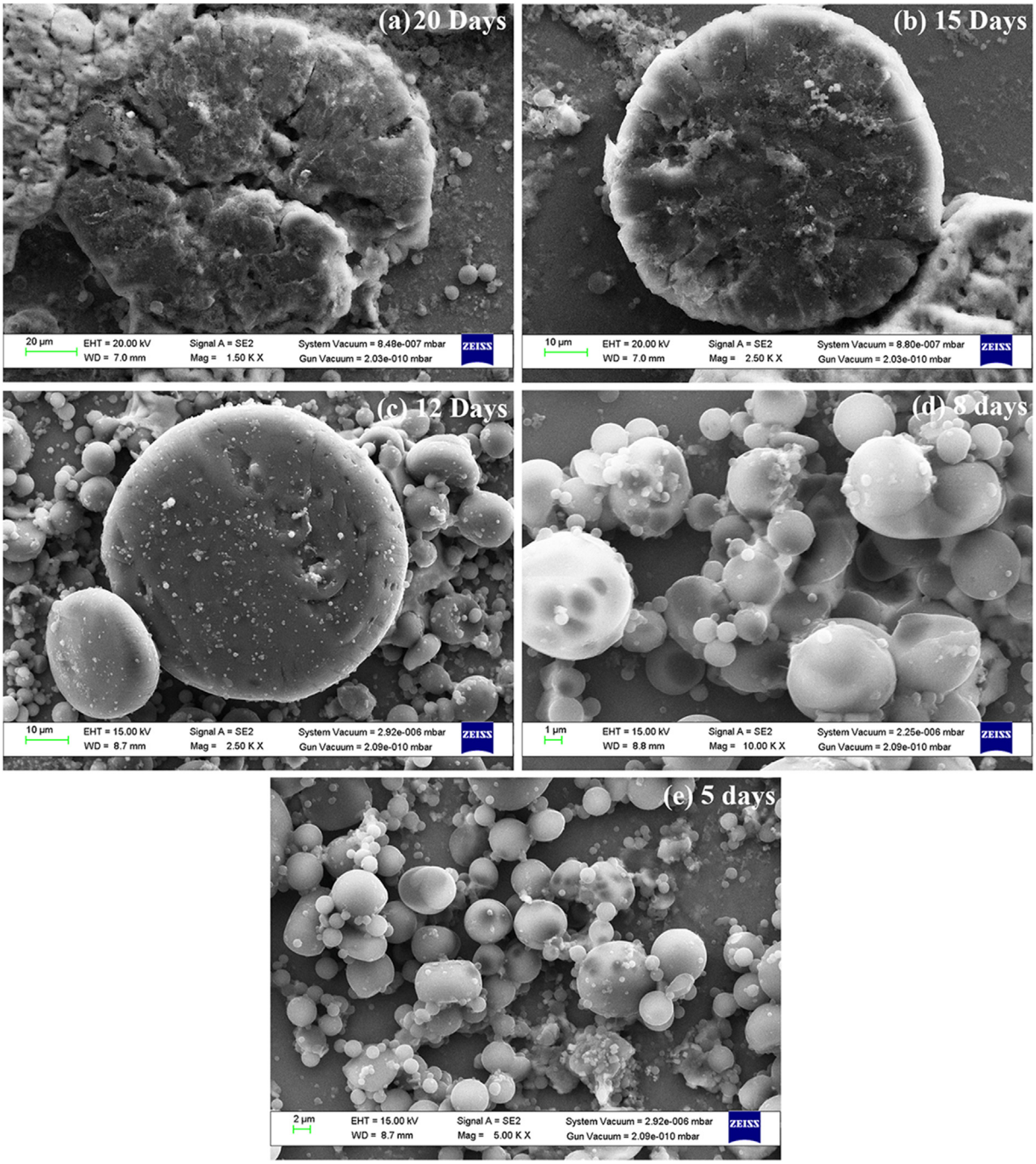

Figure 9. Degradation study of drug loaded microspheres.

NCI–H522 cell line (Human, Lung, Non-small cell lung cancer) was used and kept in RPMI-1650 complete media, and 5000 cells per well were seeded in 96 well plate.

The media was kept for 24 h, and drug dosing was performed at 0.1% v/v ethanol in the media. Here, we have prepared three different samples, i.e., Sample 1–Drug and PEG in Ethanol, Sample 2–Drug in Ethanol, and Sample 3–drug loaded microsphere.

These three samples were taken in triplicate. After 24 h of incubation, 20 µl MTT (10 mg/ml stock) was added to these samples and incubated for 4 h at 37 °C.

After the incubation is completed, absorbance at 585 nm using BMG Labtech FLUOstar OPTIMA, a microplate reader. Figure 6 shows that the self-passivated graphene quantum dots provide maximum cell viability.

The IC_{50} is the value that demonstrates how much concentration of the drug is required to minimize the binding of another drug with an enzyme by 50%. Under certain conditions, it can be used to express the affinity of the enzyme inhibitor. As mentioned in Table 1, it is clearly visible that the IC_{50} value of our final sample, i.e., drug loaded microsphere solution, is very low as compared to the other two samples.

AO/Et–Br staining was applied to identify morphological changes indicative of apoptosis in the cell nuclei. The cell nucleus of a cell is stained green by AO, a cell-permeable dye that intercalates with DNA to do so. The cells turn orange when Et–Br, in contrast, enters cells with torn plasma membranes and intercalates with double-stranded DNA. In Figure 7 NCI–H522 cell line were stained with a combination of acridine orange (AO) and ethidium bromide (Et–Br). No significant apoptosis was observed in the healthy control group, and the live cells adopted acridine

orange and green hues along with typical and healthy cell shapes, but the cells treated with IC_{50} value of Gefitinib loaded microspheres appeared with a constricted nucleus and compromised membrane appear yellowish-orange in color, signifying early or late apoptosis phases, while necrotic cells appear red.

3.6. FESEM analysis of microspheres

Surface morphology assumes to be an essential part of the drug release profile of entrapped drugs, i.e., Gefitinib in the microspheres. Size, in addition to the smooth morphology of the microspheres, governs the release characteristics of polymeric microspheres as well as the initial burst release. Smaller microspheres have a high surface area to volume ratio, i.e., they have a bigger area that will be exposed to the medium in which they are dissolved, which will influence towards the higher drug release rate. Here from Figure 8, it can be observed that synthesized microspheres are mostly in the micrometer size range; hence they have a favorable condition for small initial burst release and then followed by sustained release of drugs which is a favorable quality. Moreover, in Figure 8(a, b, c, d), the images are taken at different scales by which it can be clearly observed that the microspheres are smooth and almost spherical in shape.

3.7. Degradation study of microspheres

Figure 9 represents the close view of the degraded microspheres where the pores are clearly visible. The hydrolytic reaction took place when microspheres came into contact with PBS at pH 7.4. It can be observed that when microspheres are placed into the PBS buffer as the time passes, the formation of pores begins, and microspheres start to degrade and eventually forms clusters leaving their identical spherical structure behind. Figure 9(a) shows that the microsphere has been totally ruptured after 20 days and in Figure 9(b, c, d, e) we can see the changes in surface morphology of microspheres as the degradation process proceed with the increasing number of days.

3.8. In-vitro drug release from microspheres

The drug release rate of the Gefitinib-PEG-GQDs microsphere was done In-vitro with the help of the UV-Vis spectrophotometry technique. A calibration curve was plotted with the known drug concentration. The concentrations calculated from the standard curve were used to portray the cumulative discharge of the drug from microspheres with respect to time.

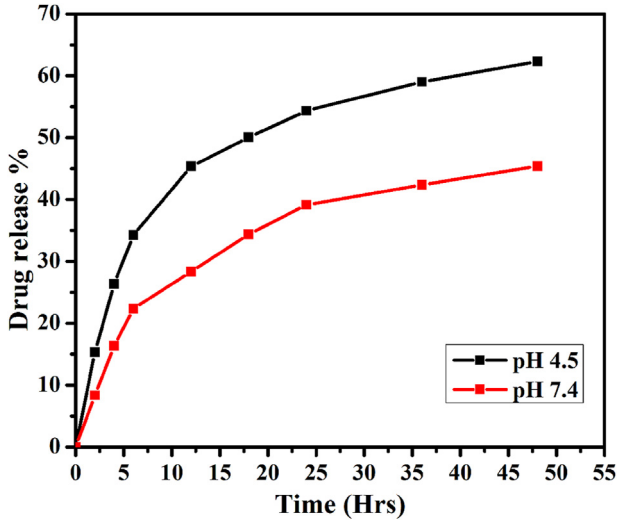

Figure 10. The in-vitro release profile for Gefitinib loaded microspheres at pH 4.5 and pH 7.4, respectively.

A drug release study is done in an acidic and basic pH environment for a comparative release study. For acidic pH, acetate buffer of pH value 4.5 was used, and for basic pH, PBS buffer solution with a 7.4 pH value was used. The time-dependent drug release profile of microspheres is shown in Figure 10. The drug release profile of Gefitinib-PEG-GQDs microspheres has shown a biphasic pattern. Initially, the release rate was rapid, which was followed by sustained release. After 48 h, the released Gefitinib was around 65% at acidic pH, i.e., 4.5 on the pH scale, which reflects the sustainable environment for the cancer cell. The quick-release of the drug in the first 48 h is suggested due to the release of the adsorbed drug on the outer shell of the microspheres. This exact mechanism for the drug release is still in debate, but our hypothesis for the same is that when the adsorbed drug is removed and the polymer surface starts degrading, then the outer layer starts acting as the permeable membrane. After the creation of a permeable outer membrane, the drug molecules start diffusing out via this layer in a controlled fashion. The brisk release of Gefitinib under acidic conditions may be because of destabilized electrostatic interactions.

At basic pH, which is similar to physiological conditions, the drug release from Gefitinib loaded microspheres was slower as compared to the acidic microenvironment, which makes them appropriate applicants for target drug delivery of cancerous cells because cancerous cells show sustainable growth only acidic environment and in the basic environment these cells can-not have sustainable growth. In this way, we can conclude that slower release in a basic environment and higher release in an acidic environment serve the purpose of targeted drug delivery capability of microspheres.

4. Conclusion

The graphene quantum dots were synthesized using PEG as source material because of their excellent biocompatibility and ethanol as a solvent because of the selected drug (Gefitinib) solubility. The fluorescence of the PEG-GQDs falls in the array of blue spectra in the VIBGYOR spectra with an excellent dispersibility insolvent. The drug (Gefitinib) was first conjugated with PEG-GQDs and then incorporated into microspheres using a single emulsification method. The main reason for choosing the single emulsification method over the double emulsification method is that by doing double emulsification, the shape and morphology of our microspheres are disturbed, and many variations in size have been seen but by using the single emulsification method, the size of microspheres was uniform and monodispersed. Hence, we can conclude that this method of drug delivery is suitable for direct delivery of the drug at the active site of lung cancer and can be more efficient than the oral drug delivery method.

Declarations

Author contribution statement

Abhishek Gautam: Conceived and designed the experiments; Performed the experiments; Analyzed and interpreted the data; Wrote the paper.

Kaushik Pal: Conceived and designed the experiments; Analyzed and interpreted the data; Contributed reagents, materials, analysis tools or data.

Funding statement

This research did not receive any specific grant from funding agencies in the public, commercial, or not-for-profit sectors.

Data availability statement

Data will be made available on request.

Declaration of interest's statement

The authors declare no conflict of interest.

Acknowledgements

The author gratefully thanks the MHRD fellowship from IIT-Roorkee for pursuing a Ph.D. The authors appreciate the valuable facility provided by the Department of Metallurgical and Materials Engineering for HRTEM analysis at IIT-Roorkee.

References

[1] W. Wang, Y. Hao, Y. Liu, R. Li, D.B. Huang, Y.Y. Pan, Nanomedicine in lung cancer: current states of overcoming drug resistance and improving cancer immunotherapy, Wiley Interdiscip. Rev. Nanomedicine Nanobiotechnology. 13 (2021) 1–22.
[2] C.Y. Huang, D.T. Ju, C.F. Chang, P. Muralidhar Reddy, B.K. Velmurugan, A review on the effects of current chemotherapy drugs and natural agents in treating non-small cell lung cancer, Biomed 7 (2017) 12–23.
[3] S.A. Brown, N. Sandhu, J. Herrmann, Systems biology approaches to adverse drug effects: the example of cardio-oncology, Nat. Rev. Clin. Oncol. 12 (2015) 718–731.
[4] N. Kolishetti, S. Dhar, P.M. Valencia, L.Q. Lin, R. Karnik, S.J. Lippard, R. Langer, O.C. Farokhzad, Engineering of self-assembled nanoparticle platform for precisely controlled combination drug therapy, Proc. Natl. Acad. Sci. U.S.A. 107 (2010) 17939–17944.
[5] M.E. Davis, Z. Chen, D.M. Shin, Nanoparticle therapeutics: an emerging treatment modality for cancer, Nat. Rev. Drug Discov. 7 (2008) 771–782.
[6] D.K. Tripathi, S. Sarkar, M.K. Meher, K.M. Poluri, Limitations in commercialization of green polymeric nanocomposites and avenues for rectification, in: Green Polymeric Nanocomposites, CRC Press, 2020, pp. 281–312.
[7] K. Rani, S. Paliwal, A review on targeted drug delivery: its entire focus on advanced therapeutics and diagnostics, Scholars J. Appl. Med. Sci. 2 (2014) 328e331.
[8] S.M. Moghimi, A.R. Rajabi-Siahboomi, Recent advances in cellular, sub-cellular and molecular targeting, Adv. Drug Deliv. Rev. 41 (2000) 129.
[9] I. Matai, A. Sachdev, P. Gopinath, Self-assembled hybrids of fluorescent carbon dots and PAMAM dendrimers for epirubicin delivery and intracellular imaging, ACS Appl. Mater. Interfaces 7 (2015) 11423–11435.
[10] A. Grigoletto, K. Maso, A. Mero, A. Rosato, O. Schiavon, G. Pasut, Drug and protein delivery by polymer conjugation, J. Drug Deliv. Sci. Technol. 32 (2016) 132–141.
[11] J. Fang, W. Islam, H. Maeda, Exploiting the dynamics of the EPR effect and strategies to improve the therapeutic effects of nanomedicines by using EPR effect enhancers, Adv. Drug Deliv. Rev. 157 (2020) 142–160.
[12] Y. Matsumura, Cancer stromal targeting therapy to overcome the pitfall of EPR effect, Adv. Drug Deliv. Rev. 154–155 (2020) 142–150.
[13] N. Kamaly, B. Yameen, J. Wu, O.C. Farokhzad, Degradable controlled-release polymers and polymeric nanoparticles: mechanisms of controlling drug release, Chem. Rev. 116 (2016) 2602–2663.
[14] S.T. Sanjay, W. Zhou, M. Dou, H. Tavakoli, L. Ma, F. Xu, X.J. Li, Recent advances of controlled drug delivery using microfluidic platforms, Adv. Drug Deliv. Rev. 128 (2018) 3–28.
[15] K. Ulbrich, K. Hola, V. Subr, A. Bakandritsos, J. Tucek, R. Zboril, Targeted drug delivery with polymers and magnetic nanoparticles: covalent and noncovalent approaches, release control, and clinical studies, Chem. Rev. 116 (2016) 5338–5431.
[16] D. Nagel, J.M. Behrendt, G.F. Chimonides, E.E. Torr, A. Devitt, A.J. Sutherland, A.V. Hine, Polymeric microspheres as protein transduction reagents, Mol. Cell. Proteomics 13 (2014) 1543–1551.
[17] A. George, P.A. Shah, P.S. Shrivastav, Natural biodegradable polymers based nano-formulations for drug delivery: a review, Int. J. Pharm. 561 (2019) 244–264.
[18] V.D. Prajapati, G.K. Jani, J.R. Kapadia, Current knowledge on biodegradable microspheres in drug delivery, Expet Opin. Drug Deliv. 12 (2015) 1283–1299.
[19] H. Lu, W. Li, H. Dong, M. Wei, Graphene quantum dots for optical bioimaging, Small 15 (2019) 1–19.
[20] D. Jiang, Y. Chen, N. Li, W. Li, Z. Wang, J. Zhu, H. Zhang, B. Liu, S. Xu, Synthesis of luminescent graphene quantum dots with high quantum yield and their toxicity study, PLoS One 10 (2015) 5–7.
[21] M.K. Kumawat, M. Thakur, R.B. Gurung, R. Srivastava, Graphene quantum dots for cell proliferation, nucleus imaging, and photoluminescent sensing applications, Sci. Rep. 7 (2017) 1–16.
[22] J. Shen, Y. Zhu, X. Yang, J. Zong, J. Zhang, C. Li, One-pot hydrothermal synthesis of graphene quantum dots surface-passivated by polyethylene glycol and their photoelectric conversion under near-infrared light, New J. Chem. 36 (2012) 97–101.
[23] M.L. Liu, L. Yang, R.S. Li, B. Bin Chen, H. Liu, C.Z. Huang, Large-scale simultaneous synthesis of highly photoluminescent green amorphous carbon nanodots and yellow crystalline graphene quantum dots at room temperature, Green Chem. 19 (2017) 3611–3617.
[24] S. Bak, D. Kim, H. Lee, Graphene quantum dots and their possible energy applications: a review, Curr. Appl. Phys. 16 (2016) 1192–1201.
[25] C. Zhao, X. Song, Y. Liu, Y. Fu, L. Ye, N. Wang, F. Wang, L. Li, M. Mohammadniaei, M. Zhang, Q. Zhang, J. Liu, Synthesis of Graphene Quantum Dots and Their Applications in Drug Delivery 18, 2020, pp. 1–32.
[26] Y. Shi, C. Su, W. Cui, H. Li, L. Liu, B. Feng, M. Liu, R. Su, L. Zhao, Gefitinib loaded folate decorated bovine serum albumin conjugated carboxymethyl-betacyclodextrin nanoparticles enhance drug delivery and attenuate autophagy in folate receptor-positive cancer cells, J. Nanobiotechnol. 12 (2014) 1–11.
[27] J. Li, M. Zhao, P. He, M. Hidalgo, S.D. Baker, Differential metabolism of gefitinib and erlotinib by human cytochrome P450 enzymes, Clin. Cancer Res. 13 (2007) 3731–3737.
[28] Q. Lin, G. Liu, Z. Zhao, D. Wei, J. Pang, Y. Jiang, Design of gefitinib-loaded poly (L-lactic acid) microspheres via a supercritical anti-solvent process for dry powder inhalation, Int. J. Pharm. 532 (2017) 573–580.
[29] A.I. Kuruppu, L. Zhang, H. Collins, L. Turyanska, N.R. Thomas, T.D. Bradshaw, An apoferritin-based drug delivery system for the tyrosine kinase inhibitor gefitinib, Adv. Healthc. Mater. 4 (2015) 2816–2821.
[30] S. Watanabe, J. Tanaka, T. Ota, R. Kondo, H. Tanaka, H. Kagamu, K. Ichikawa, J. Koshio, J. Baba, T. Miyabayashi, I. Narita, H. Yoshizawa, Clinical responses to EGFR-tyrosine kinase inhibitor retreatment in non-small cell lung cancer patients who benefited from prior effective gefitinib therapy: a retrospective analysis 11, 2011, pp. 1–7.
[31] B. Singh, P. Singh, A.J. Sutherland, K. Pal, Control of shape and size of poly (lactic acid) microspheres based on surfactant and polymer concentration, Mater. Lett. 195 (2017) 48–51.
[32] S.B. Patil, S.Z. Inamdar, K.R. Reddy, A.V. Raghu, K.G. Akamanchi, A.C. Inamadar, R.V. Kulkarni, Functionally tailored electro-sensitive poly (acrylamide)-g-pectin copolymer hydrogel for transdermal drug delivery application: synthesis, characterization, in-vitro and ex-vivo evaluation, Drug Deliv. Lett. 10 (3) (2020) 185–196.
[33] P.V. Kulkarni, C.A. Roney, P. Antich, F.J. Bonte, A.V. Raghu, T.M. Aminabhavi, Quinoline-n-butylcyanoacrylate-based nanoparticles for brain targeting for the diagnosis of Alzheimer's disease, Wiley Interdiscip. Rev. Nanomed. Nanobiotechnol 21 (2010) 35–47.
[34] A.V. Raghu, H.M. Jeong, Synthesis, characterization of novel dihydrazide containing polyurethanes based on N1, N2-bis [(4-hydroxyphenyl) methylene] ethanedihydrazide and various diisocyanates, J. Appl. Polym. Sci. 107 (5) (2008) 3401–3407.
[35] A.V. Raghu, G. Anita, Y.M. Barigaddi, G.S. Gadaginamath, T.M. Aminabhavi, Synthesis and characterization of novel polyurethanes based on 2, 6-bis (4-hydroxybenzylidene) cyclohexanone hard segments, J. Appl. Polym. Sci. 104 (1) (2007) 81–88.